ON THE ARTIFICIAL COMPRESSION METHOD FOR SECOND-ORDER NONOSCILLATORY CENTRAL DIFFERENCE SCHEMES FOR SYSTEMS OF CONSERVATION LAWS

KNUT–ANDREAS LIE AND SEBASTIAN NOELLE

ABSTRACT. The recently proposed high-order central difference schemes for conservation laws have a tendency of smearing linear discontinuities. In principle, Harten's artificial compression method (ACM) could be used to improve resolution. We analyse why this approach has not yet been used successfully and derive a more powerful version of the ACM based on a rigorous estimate of the total variation. We discuss the potential danger of overcompression and point out directions of future algorithmic development.

1. INTRODUCTION

The most successful and popular methods for computing solutions of hyperbolic systems of conservation laws are the upwind schemes originated by Godunov (1959) [4] and extended to second-order accuracy by van Leer (1979) [23]. A one-dimensional characteristic decomposition of the data makes it possible to update each wave-component of the solution in a stable and accurate manner. An alternative to the Godunov-type upwind schemes is the Lax–Friedrichs central difference scheme, first introduced in 1954 by Lax [11], which was extended to second-order accuracy by Nessyahu and Tadmor in 1990 [17]. Since central schemes apply no characteristic information or Riemann solvers, they yield compact, efficient computer code and can in principle be used as black-box solvers. This attractive simplicity has lead to a widespread revival of the central schemes; see for example [16, 13] (third and fourth order), [1, 7] (two-dimensional Cartesian grids), [3, 2] (two-dimensional triangular grids), [10, 8] (non-staggered grids), and [15, 19, 22] (applications to relaxation systems, semiconductors, granular flows).

Numerical experiments in [17] show that the Lax–Friedrichs-type second-order central difference schemes resolve both smooth waves and shocks (almost) as sharply as comparable second-order upwind schemes. On the other hand, a common criticism of second-order central difference schemes is that they smear *linear* discontinuities more than Godunov-type upwind schemes. Already in their original paper, Nessyahu and Tadmor [17] suggest two compression techniques to improve the resolution of linear waves:

The first version is a corrector step suggested by Harten which basically solves an inverse diffusion equation after every time-step. Since this step is applied to the full system, it may prevent the physically correct spreading of rarefaction waves. This may lead to entropy violating shocks.

The second technique - also inspired by Harten [5, 6] - starts with a Roe-type characteristic decomposition of the numerical data [18]. A switch function should detect corners of linear discontinuities. Near these corners, a steeper (i.e., compressive) reconstruction is applied to

the linear fields only. In the following, we will call this approach the artificial compression method (ACM). The advantage of ACM over the inverse diffusion technique is that it avoids entropy violating shocks, which can only occur in the nonlinear fields.

In their paper [17], Nessyahu and Tadmor do not show numerical experiments with this second version of ACM. This gap is the starting point of the present paper.

In the following we will analyse the ACM for the linear scalar advection equation. We show that in this context it is equivalent to the standard second-order Nessyahu-Tadmor scheme with a certain limiter function. This limiter is a special case of a one-parameter family of limiters. Another member of this family is van Leer's limiter function, which is *not* compressive. We show that Harten's version of ACM as described in [17] is even *less* compressive than van Leer's limiter.

A sharp estimate of the total variation (TV) allows us to derive the range of TVD (TV diminishing) limiters, among them limiters that are much more compressive than van Leer's. Numerical experiments confirm the impressive power of these limiters.

However, this is not the end of the story: the power of the ACM is also its potential weakness. Smooth linear waves may be overcompressed into piecewise linear ones with sharp corners, or even into step functions. The class of limiters used, which depends on the quotient of left-sided and right-sided differences of the cell averages, cannot distinguish between corners of a step, where compression should be applied, and smooth extrema, where it should not be used.

We would like to mention that for the non-staggered central-upwind scheme [8], Kurganov and Petrova [9] have developed a different technique to sharpen linear waves, but they have not discussed the risk of overcompression for their approach. Our approach is more closely related to the one analyzed by Sweby [21] in the context of upwind schemes, and our numerical results and conclusions are comparable to his.

The outline of the paper is as follows. In Section 2 we derive suffient TVD conditions for second order central schemes using Sweby-type limiters for the linear advection equation. In Section 3, we show that for the linear advection problem, Harten's ACM falls into the class of schemes considered in Section 2, so the TVD-conditions derived there can be used to increase the compression of the ACM while preserving TVD stability. In Section 4, we single out a parameter which seems to allow a classification of limiters into dissipative, well-balanced, compressive and overcompressive ones. We propose a class of modified Superbee limiters based on this parameter. Numerical experiments, both for central and upwind schemes, back up the suggested classification. In Section 5, we presenpresent numerical experiments for the system of the Euler equations which show remarkable resolution of rapidly varying linear waves. We conclude our paper by pointing out directions for future algorithmic improvement in Section 6.

2. TVD ANALYSIS FOR CENTRAL DIFFERENCE SCHEMES

To make our point as transparent as possible, we assume that the standard characteristic decomposition has already been carried out. Hence we restrict our attention to the one-dimensional, linear, scalar advection equation

$$(1) \qquad\qquad u_t + f(u)_x = 0, \quad f(u) = au.$$

The NT (Nessyahu-Tadmor) scheme can be written in the general conservative staggered form

$$(2) \qquad\qquad u_{i+\frac{1}{2}}^{n+1} = \frac{1}{2}(u_i^n + u_{i+1}^n) - \lambda(g_{i+1}^n - g_i^n)$$

where u_i^n approximates the cell average over the ith cell $[(i-\frac{1}{2})\Delta x, (i+\frac{1}{2})\Delta x]$ at time $t^n = n\Delta t$, the update $u_{i+\frac{1}{2}}^{n+1}$ approximates the cell average over the staggered cell $[i\Delta x, (i+1)\Delta x]$ at time t^{n+1} and the numerical fluxes are

$$(3) \qquad g_i^n = f(u_i^{n+\frac{1}{2}}) + \frac{1}{8\lambda}u_i'.$$

Here $\lambda = \frac{\Delta t}{\Delta x}$ and $u_i^{n+\frac{1}{2}}$ is an intermediate value obtained by the predictor step

$$(4) \qquad u_i^{n+\frac{1}{2}} = u_i^n - \frac{\lambda}{2}f_i'.$$

The values u_i' and f_i' are numerical approximations of the derivatives $\Delta x u_x$ and $\Delta x f(u)_x$ over the ith cell at time t^n and will be specified below.

The following Lemma of Nessyahu and Tadmor carries over Harten's TVD result [6, Lemma 2.2] to the staggered schemes:

Lemma 1. *The scheme (2)–(4) is TVD if*

$$(5) \qquad \lambda|g_{i+1} - g_i| \le \frac{1}{2}|u_{i+1} - u_i|.$$

For the proof, see [17, Lemma 3.1]. Here and in the following we omit the superscript n if no misunderstanding is possible. Now let

$$\nu := \lambda a$$

be the Courant number. Throughout the following, we always assume that the time-step satisfies the Courant–Friedrichs–Lewy (CFL) condition

$$(6) \qquad |\nu| \le \frac{1}{2}.$$

Note that (5) is the discrete analog of (6). Now we use the linearity of the flux function to simplify the scheme:

$$u_i^{n+\frac{1}{2}} = u_i^n - \frac{\nu}{2}u_i'$$

and

$$(7) \qquad \lambda g_i^n = \nu u_i^n + \frac{1 - 4\nu^2}{8}u_i'.$$

Therefore,

$$\lambda(g_{i+1}^n - g_i^n) = \left(\nu + \frac{1 - 4\nu^2}{8}\frac{u_{i+1}' - u_i'}{u_{i+1} - u_i}\right)(u_{i+1} - u_i).$$

Lemma 1 implies that the scheme (2), (7), will be TVD provided that

$$(8) \qquad \left|\nu + \frac{1 - 4\nu^2}{8}\frac{u_{i+1}' - u_i'}{u_{i+1} - u_i}\right| \le \frac{1}{2}.$$

In the following we consider reconstructions of the form

$$(9) \qquad u_i' = \phi(r_i)(u_i - u_{i-1}).$$

where

$$(10) \qquad r_i = \frac{u_{i+1} - u_i}{u_i - u_{i-1}}.$$

The Lipschitz-continuous function ϕ is called the limiter; see Sweby (1984) [21]. We will sometimes call it a Sweby-type limiter to stress that it depends only on the ratio r_i. We require that the limiters satisfy the symmetry condition

$$(11) \qquad\qquad \phi(r) = r\phi\Big(\frac{1}{r}\Big).$$

Therefore, we can also express the numerical derivative u_i' in terms of the right-sided differences,

$$(12) \qquad\qquad u_i' = \phi\left(\frac{1}{r_i}\right)(u_{i+1} - u_i).$$

Lemma 2. *The scheme* (2), (7), (9) *is TVD if*

$$(13) \qquad\qquad \phi(r) = 0 \quad \text{for} \quad r \leq 0$$

and

$$(14) \qquad\qquad 0 \leq \phi(r) \leq \frac{4}{1+2|\nu|}\min(r,1) \quad \text{for} \quad r > 0.$$

Conditions (13)–(14) are the staggered-grid analogue of Sweby's TVD-condition [21, eq. (3.12)].

Proof. Suppose that $u_i^n = u_{i+1}^n$. In this case (9) and (12) imply that $u_i' = u_{i+1}' = 0$ and hence $g_i^n = g_{i+1}^n$. This implies (5).

Now suppose $u_i^n \neq u_{i+1}^n$. We will verify that (13) and (14) imply (8). From (9) and (12)

$$\frac{u_{i+1}'}{u_{i+1} - u_i} = \phi(r_{i+1}).$$

and

$$\frac{u_i'}{u_{i+1} - u_i} = \phi\left(\frac{1}{r_i}\right)$$

From (13) and (14),

$$0 \leq \phi(r_{i+1}), \phi\left(\frac{1}{r_i}\right) \leq \frac{4}{1+2|\nu|},$$

so

$$\left|\frac{u_{i+1}' - u_i'}{u_{i+1} - u_i}\right| = \left|\phi(r_{i+1}) - \phi\left(\frac{1}{r_i}\right)\right|$$

$$\leq \max\left(\phi(r_{i+1}), \phi\left(\frac{1}{r_i}\right)\right)$$

$$\leq \frac{4}{1+2|\nu|},$$

and

$$\left|\nu + \frac{1 - 4\nu^2}{8}\frac{u_{i+1}' - u_i'}{u_{i+1} - u_i}\right| \leq |\nu| + \frac{(1 - 2|\nu|)(1 + 2|\nu|)}{8}\frac{4}{1+2|\nu|}$$

$$= |\nu| + \frac{1}{2} - |\nu| = \frac{1}{2}.$$

This implies (8) and hence the TVD-property. $\square$

If we set $4/(1+2|\nu|)$ to its minimal value of 2 (obtained for $|\nu| = 0.5$), then these conditions coincide with the TVD-constraints of Sweby for non-staggered schemes. Recall that these limiters lead to second-order accurate schemes away from extrema if
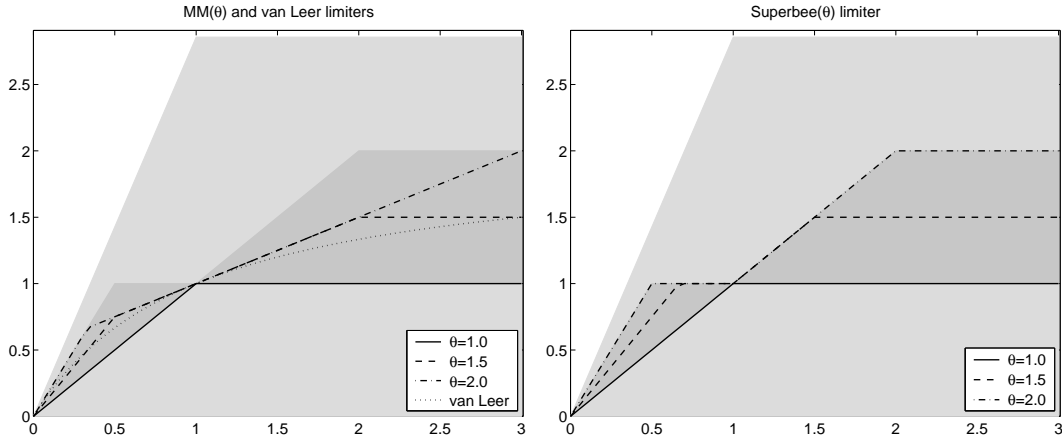
$$(15) \qquad\qquad \phi(1) = 1.$$

FIGURE 1. Sketch of MM, VL and SB limiters. Light shaded area gives TVD region for $\nu = 0.2$ (see Lemma 2) and dark shaded area "the second order TVD" region of Sweby.

To this, we would like to add the stricter accuracy condition

$$(16) \qquad (\phi(r) - 1)(\phi(r) - r) \leq 0,$$

which is equivalent to requesting that the resulting slope will be a convex combination of the left-sided and right-sided difference quotients. Of course, (16) implies (15). Examples of second-order accurate TVD limiters are van Leer's limiter (VL),

$$(17) \qquad \phi^{VL}(r) := \frac{r + |r|}{1 + |r|},$$

the family of MinMod limiters (MM$_\theta$)

$$(18) \qquad \phi_\theta^{MM}(r) := \max\{0, \min\{\theta r, \frac{1 + r}{2}, \theta\}\},$$

for $1 \leq \theta \leq 4/(1 + 2|\nu|)$, and the family of Superbee limiters (SB$_\theta$)

$$(19) \qquad \phi_\theta^{SB}(r) := \max\{0, \min\{\theta r, 1\}, \min\{r, \theta\}\},$$

again for $1 \leq \theta \leq 4/(1 + 2|\nu|)$. All these limiters are plotted in Figure 1 along with the "second order TVD" region of Sweby and the TVD region of Lemma 2.

In Figure 2 we show the approximation to the solution of the linear advection equation (1) with $a = 1$ and periodic initial data on the unit interval. The approximations are computed using various limiters and CFL-number $\nu = 0.2$. The initial data in the left column is the step function

$$u_0(x) := \begin{cases} 1 & \text{for} \quad 0 \leq x < 0.5 \\ 3 & \text{for} \quad 0.5 \leq x < 1 \end{cases}$$

and in the right column the sine wave

$$u_0(x) := 2 + \sin(2\pi x).$$

Note that while it may be desirable to choose a larger CFL number, say 0.4, for the problem at hand, the lower CFL number here is motivated from gas dynamics. There the time-step is calculated using the fastest wave speed, which occurs in the nonlinear acoustic wave. If the Mach number is around unity (i.e., $|v| \approx c$), then the speed $|v|$ of the linear field is only half that of the faster nonlinear speed $|v| + c$, so the effective CFL number for the linear field will
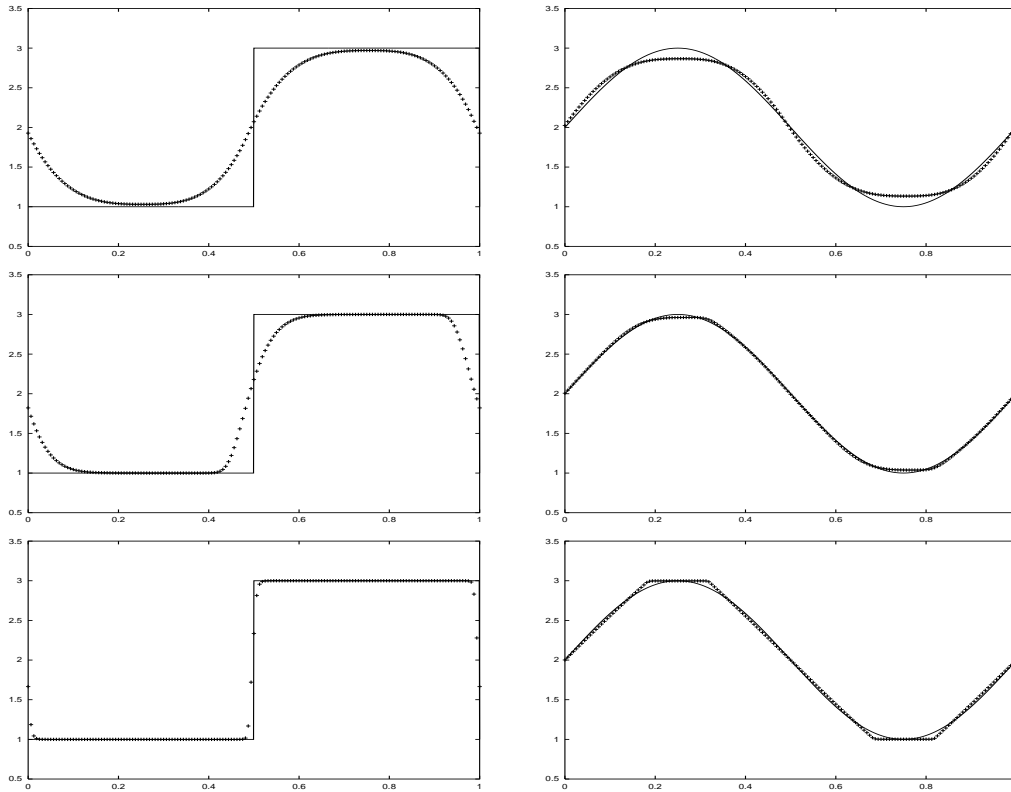
FIGURE 2. Computations of a periodic step (left column) and a sine wave (right column) using various limiters. 160 points, 20 periods (16.000 time-steps), CFL = 0.2. From top to bottom: MM_1, VL, SB_2.

be only one half that of the overall algorithm. We compute 20 temporal periods using 160 grid points. This corresponds to 16.000 time-steps.

Clearly, all computations are total-variation stable. For the MM (= MM_1) and VL limiters the numerical results are dominated by dissipation. After 20 periods, the step resembles a steep, but smooth wave. As time proceeds, the solution will become more and more smeared. Compare the results for the SB (= SB_2) limiter. Here the step is resolved within a few mesh-points, and it does not spread with time. On the other hand, the smooth sine wave has developed two corners near the extrema for the SB limiters. Clearly, the challenge lies in designing reconstructions that work well both for smooth and discontinuous solutions.

3. HARTEN'S ARTIFICIAL COMPRESSION METHOD (ACM)

The question of designing reconstructions that work well both for smooth and discontinuous solutions was treated in 1983 by Harten [6]. In his artificial compression method (ACM) he starts the reconstruction with the standard MinMod (MM) limiter. To this, he adds an additional contribution near the corners of a jump-discontinuity, making the limiter compressive. The core of the ACM is a switch-function that quantifies how much compression may be used. The resulting reconstruction reads

$$(20) \qquad u_i' = MM(u_{i+1} - u_i, u_i - u_{i-1}) + \theta_i MM(\sigma_{i+\frac{1}{2}}(u_{i+1} - u_i), \sigma_{i-\frac{1}{2}}(u_i - u_{i-1}))$$

where $\mathrm{MM}(a, b) := \phi_1^{MM}(\frac{a}{b}) \cdot b$. The switch θ_i is given by

$$\theta_i = \frac{|u_{i+1} - 2u_i + u_{i-1}|}{|u_{i+1} - u_i| + |u_i - u_{i-1}|}. \tag{21}$$

The parameters $\sigma_{i+\frac{1}{2}}$ are given as

$$\sigma_{i+\frac{1}{2}} = \sigma(\nu_{i+\frac{1}{2}}),$$

where $\nu_{i+\frac{1}{2}}$ is the local CFL number. In the linear advection case considered in this section, $\nu_{i+\frac{1}{2}} \equiv \nu$. In order to obtain a TVD bound for his scheme, Harten [6, eq.(5.1)] requests that

$$0 \le \sigma(\nu) \le 1 - |\nu| - \frac{1}{2}(Q(\nu) - |\nu|^2).$$

Here $Q(\nu)$ is the numerical viscosity of the basic numerical function used. Typical values are $Q(\nu) = |\nu|$ or $Q(\nu) = |\nu|^2$, the latter being the viscosity of the Lax–Wendroff flux. In any case, $Q(\nu) \ge |\nu|^2$.

Harten suggests to use

$$\sigma(\nu) = \frac{1}{2}(1 - Q(\nu)).$$

In particular, this gives

$$\sigma(\nu) \le \frac{1}{2}(1 - |\nu|^2) < \frac{1}{2} \quad \text{for} \quad \nu \ne 0. \tag{22}$$

Remark 3. *Note that the addition of artificial compression does not destroy the formal second-order accuracy of the underlying TVD-scheme, because θ_i is $O(\Delta x)$ in smooth parts of the solution away from the extrema. Near extrema $\theta_i = O(1)$, but at extrema TVD schemes can only be first-order accurate anyway.*

We now use Lemma 2 to derive a less restrictive TVD condition on $\sigma(\nu)$. Let r_i be given by (10). From (21) we obtain

$$\theta_i = \frac{|1 - r_i|}{1 + |r_i|}.$$

Due to the symmetry assumption (11), we may restrict the discussion to the case $0 \le r \le 1$, so $\phi_1^{MM}(r) \equiv r$. Therefore, the reconstruction (20) becomes

$$u_i' = \phi_\sigma^{ACM}(r_i)(u_i - u_{i-1}) \tag{23}$$

with

$$\phi_\sigma^{ACM}(r) = r + \frac{1 - r}{1 + r}\sigma(\nu)r. \tag{24}$$

According to Lemma 2 this reconstruction will be TVD if

$$0 \le \phi_\sigma^{ACM}(r) \le \frac{4r}{1 + 2|\nu|}.$$

In terms of the function $\sigma(\nu)$, this reads

$$0 \le \sigma(\nu) \le \frac{1 + r}{1 - r}\left(\frac{4}{1 + 2|\nu|} - 1\right).$$

Taking the minimum of the right-hand-side of this inequality over $r \in [0, 1]$ we obtain the following sufficient condition:

Lemma 4. *The reconstruction* (23) *and* (24) *is TVD provided that*

$$(25) \qquad\qquad 0 \le \sigma(\nu) \le \frac{4}{1 + 2|\nu|} - 1 =: \sigma_{max}(\nu).$$

Note that

$$1 \le \sigma_{max}(\nu) \le 3 \quad \text{for} \quad |\nu| \le \frac{1}{2}$$

which is two to six times as much as the value of $\sigma(\nu) < \frac{1}{2}$ admitted by (22)! We will use this freedom to derive a scheme that is more compressive than the one suggested by Nessyahu and Tadmor. Suppose first that we would like to construct a TVD-limiter that is independent of the local value of ν. In this case we minimize the right-hand-side of (25) over $\nu \in [0, \frac{1}{2}]$ and obtain

$$\sigma(\nu) \equiv 1.$$

Remark 5. *It can easily be checked that for* $\sigma = 1$,

$$\phi_{\sigma=1}^{ACM}(r) = r + \frac{1-r}{1+r}r = \frac{2r}{1+r} = \phi^{VL}(r)$$

so we recover van Leer's limiter function.

Note that the direct application of Harten's ACM (20), (21) to the scalar linear advection equation (1) with the constraint $\sigma < 1/2$ (see equation (22)) would lead to a piecewise linear reconstruction which would be less steep than van Leer's. The resulting "ACM" scheme would smear linear discontinuities considerably more than the second order scheme using van Leer's limiter. Therefore, if we want to have any chance of resolving a discontinuous solution within a few mesh points in the large time range, we have to go to higher values of σ. For

$$1 \le \sigma \le \sigma_{max}(\nu)$$

the family of ACM- limiters may be rewritten as

$$(26) \qquad \phi_\sigma^{ACM}(r) = \begin{cases} 0 & \text{for} \quad r \le 0 \\ \frac{r(\sigma+1) - r^2(\sigma-1)}{r+1} & \text{for} \quad 0 < r \le 1 \\ \frac{r(\sigma+1) - (\sigma-1)}{r+1} & \text{for} \quad r > 1 \end{cases}$$

For $\sigma \le 2$, $\phi_\sigma^{ACM}(r)$ is still monotone as a function of r, but it becomes non-monotone as σ takes values higher than 2; see Figure 3.

In Figure 4, we show numerical results for our family of ACM limiters. Clearly, we see the compressive effect as σ increases from the van Leer value of unity to larger values. Note that for $\nu = 0.2$, $\sigma_{max}(\nu) = 1.867 < 2$, so the limiter is still monotone as a function of r. Note that these results are more dissipative than those using the Superbee limiter in Figure 2. In Figure 5 we show the result for $\nu = 0.05$ and $\sigma = \sigma_{max}(\nu) = 2.6364$. With these parameters, the sine wave is compressed into a step function.

4. On a classification of Sweby-type TVD limiter functions

In the previous section, we have shown that for the prototype scalar linear advection equation, Harten's ACM reconstruction is based on a particular Sweby-type limiter. Therefore the TVD-analysis of Section 2 could be applied to steepen the reconstruction while maintaining the TVD-property.

We have seen in Sections 2 and 3 that some limiters like ϕ^{SB} or ϕ_σ^{ACM} with large σ may overcompress smooth linear waves. It would be useful to have a criterion which makes it
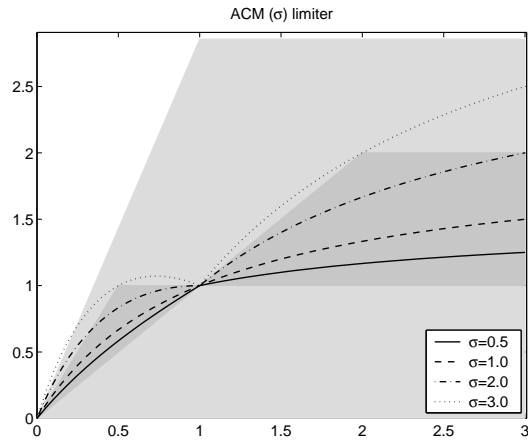
FIGURE 3. Sketch of the family of ACM limiters ϕ_σ^{ACM} (see (26)) for $\sigma = 0.5, 1.0, 2.0, 3.0$. Light shaded area gives TVD region for $\nu = 0.2$ (see Lemma 2) and dark shaded area "the second order TVD" region of Sweby.
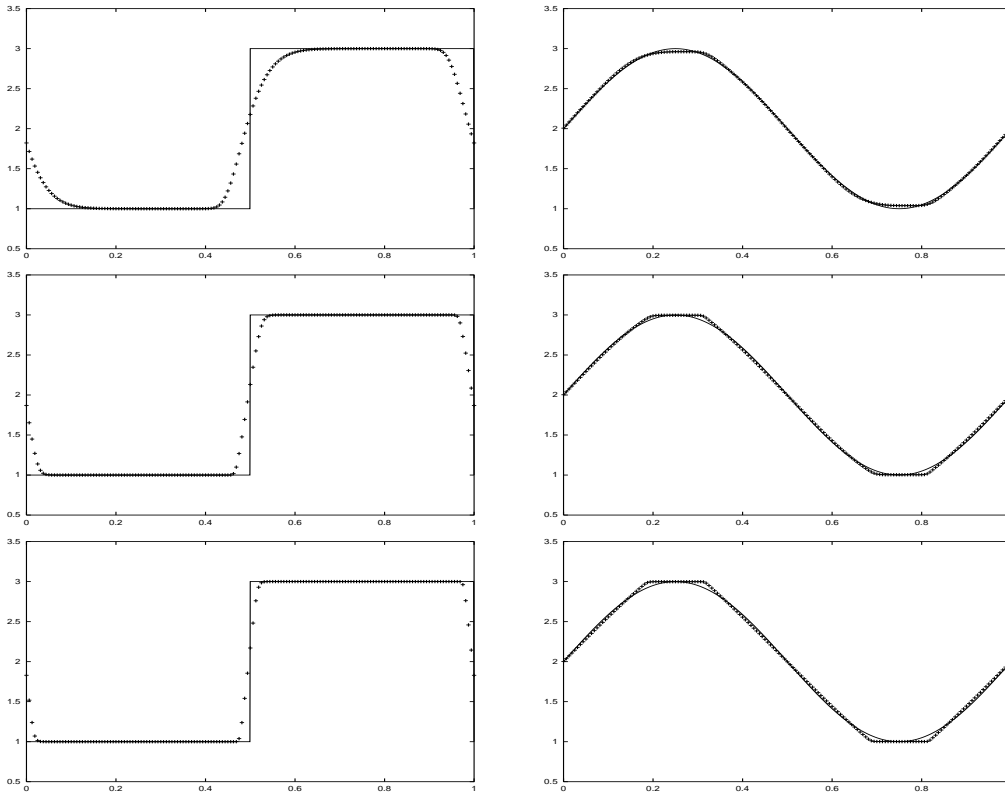

FIGURE 4. Same computation as in Figure 2, but using Harten's ACM limiter ϕ_σ^{ACM} (see (26)) with $\nu = 0.2$ and $\sigma = 1, 1.5, \sigma_{max}(\nu) = 1.857$.
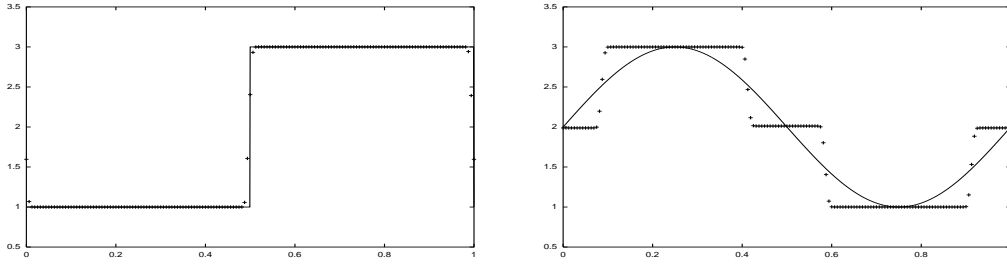
FIGURE 5. Same computation as in Figures 2 and 4, but using ϕ_σ^{ACM} with $\nu = 0.05$ and $\sigma = \sigma_{max}(\nu) = 2.636$.

possible to decide if a limiter carries this risk of overcompression, without having to run a sequence of numerical experiments like those displayed in Figures 2, 4 and 5.

In the following, we suggest such a criterion. We formulate it as a conjecture and back it up by numerical experiments with a new class of limiters which is directly derived from our criterion.

Any second order accurate limiter should be Lipschitz continuous and satisfy (15), i.e., $\phi(1) = 1$. We conjecture that the compressive character of the limiter can be classified by the magnitude of the (one-sided) derivative of ϕ at $r = 1$. Note that the symmetry condition (11) implies that

$$\phi'(r) = \phi\left(\frac{1}{r}\right) - \frac{1}{r}\phi'\left(\frac{1}{r}\right),$$

so

$$\lim_{r \to 1-} \phi'(r) = 1 - \lim_{r \to 1+} \phi'(r).$$

Classification 6. *Based on the numerical evidence accumulated so far, we would like to suggest to call a limiter*

    (i) *dissipative if* $\lim_{r \to 1-} \phi'(r) \geq \frac{1}{2}$,

    (ii) *well-balanced if* $\lim_{r \to 1-} \phi'(r) = \frac{1}{2}$,

    (iii) *compressive if* $\lim_{r \to 1-} \phi'(r) < \frac{1}{2}$,

    (iv) *overcompressive if* $\lim_{r \to 1-} \phi'(r) < 0$,

The idea is to call a limiter compressive (resp. dissipative) if away from extrema of the solution, the resulting reconstruction is steeper (resp. less steep) than the centered difference quotient.

For a well-balanced limiter left- and right-sided derivatives coincide at $r = 1$, and $\phi'(1) = \frac{1}{2}$. Note also that overcompressive limiters which satisfy the accuracy requirement (15) will always violate the stricter accuracy requirement (16).

According to this terminology,

    (i) the MinMod1 limiter and the limiter that results from Nessyahu and Tadmor's adaptation of Harten's ACM are both dissipative.

    (ii) van Leer's limiter as well as the MinMod limiters for $\theta > 1$ are well-balanced,

    (iii) the family of Superbee limiters is compressive for $\theta > 1$,

    (iv) the ACM limiters ϕ_σ^{ACM} are compressive for $1 < \sigma \leq 2$ and overcompressive for $\sigma > 2$.
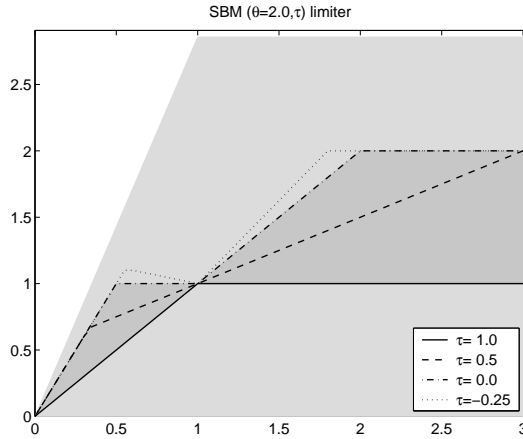
FIGURE 6. Sketch of the family of SBM limiters for $\theta = 2.0$ and $\tau = 1.0, 0.5, 0.0, -0.25$. Light shaded area gives TVD region for $\nu = 0.2$ (see Lemma 2) and dark shaded area "the second order TVD" region of Sweby.

This classification is in agreement with the numerical results displayed in Figures 2, 4 and 5.

To back up this classification further, we would like to introduce a modified family of Superbee limiters that explicitly contains the parameter $\tau = \lim\limits_{r \to 1-} \phi'(r)$

$$(27) \qquad \phi_{\theta,\tau}^{SBM}(r) := \begin{cases} 0 & \text{for } r \leq 0 \\ \min\{r\theta, 1 + \tau(r-1)\} & \text{for } 0 < r \leq 1 \\ r\phi_{\theta,\tau}^{SBM}(\frac{1}{r}) & \text{for } 1 < r \end{cases}$$

where $\tau \leq 1 \leq \theta$. Note that

$$\begin{aligned} \phi_{\theta,1}^{SBM} &= \phi_1^{MM} \\ \phi_{\theta,\frac{1}{2}}^{SBM} &= \phi_\theta^{MM} \\ \phi_{\theta,0}^{SBM} &= \phi_\theta^{SB} \end{aligned}$$

The new limiter becomes overcompressive for negative values of τ. Figure 6 contains a sketch of this limiter for $\theta = 2$ and $\tau = 1.0, 0.5, 0.0, -0.25$.

In Figure 7 we display numerical results for $\theta = 2$ and $\tau = 1.0, 0.5, 0.0, -0.25$. The effects of dissipation (for $\tau = 1.0$, MM_1 case, see also $\tau = 0.5$), compression ($\tau = 0.0$, SB_2 case) and overcompression ($\tau = -0.25$) are clearly distinguishable: for smooth data the compressive SBM limiter leads to kinks, i.e., jumps in the first derivative of the numerical solution, while the overcompressive limiter leads to jumps in the solution itself.

To demonstrate that the classification of limiters also applies to upwind schemes, we have implemented the simplest possible second order TVD-upwind scheme for the linear advection equation (1),

$$(28) \qquad u_i^{n+1} = u_i^n - \nu\big(u_i^n - u_{i-1}^n\big) - \tfrac{1}{2}\nu(1-\nu)\big(u_i' - u_{i-1}'\big),$$

where u_i' is defined by (9) as before. This is the scheme analyzed by Sweby [21, eq.(3.6)] (see also LeVeque's book [12, eq.(16.45)]). Analogously to the central scheme (see Lemma 2) one can show that the upwind scheme (28) is TVD provided that $\phi(r) = 0$ for $r \leq 0$ and

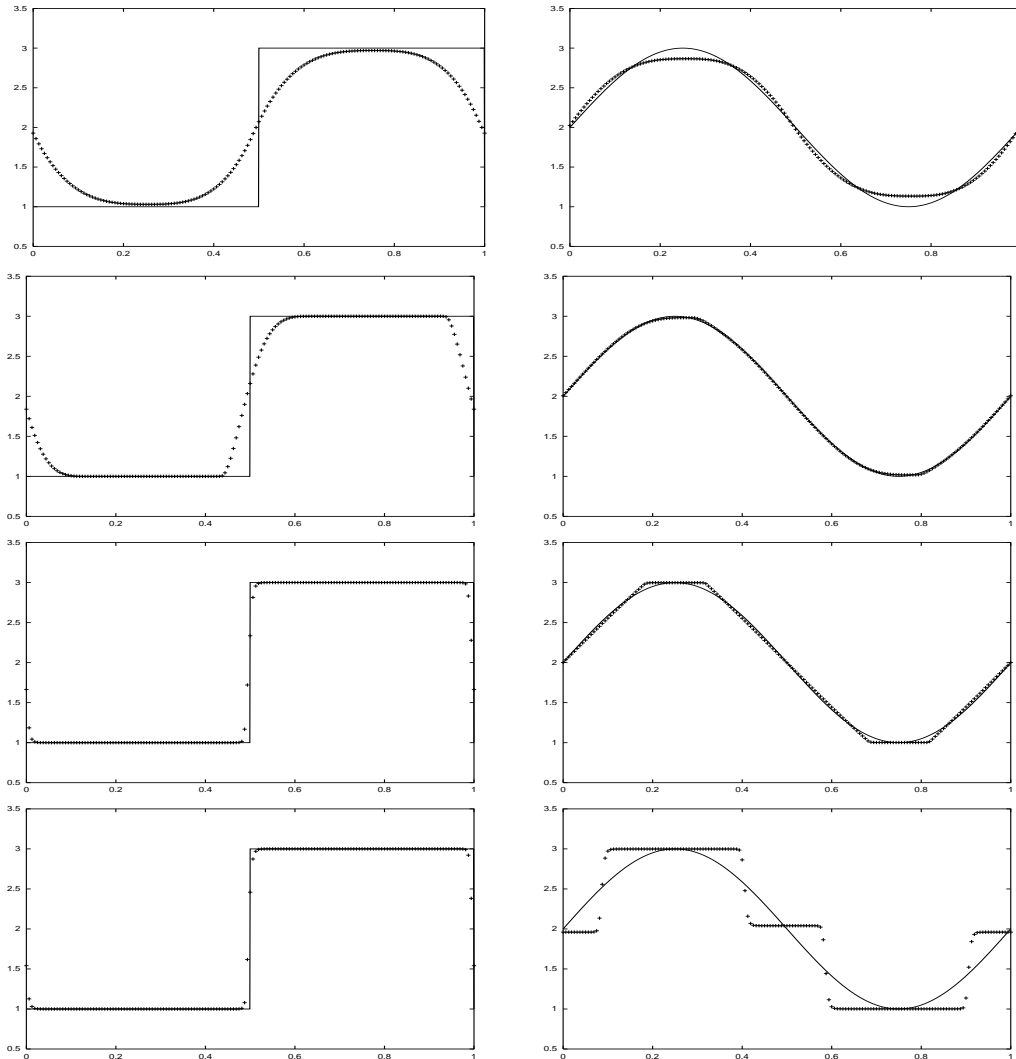$$0 \leq \phi(r) \leq \frac{2\min(1, r)}{\max(\nu, 1-\nu)} \quad \text{for } 0 \leq \nu \leq 1.$$

FIGURE 7. Same computation as in Figures 2 and 4, but using SBM limiter $\phi_{\theta,\tau}^{SBM}$ with $\theta = 2.0$ and $\tau = 1.0, 0.5, 0.0, -0.25$ (from top to bottom).

In Figure 8 we display numerical results analogous to Figure 7 for this TVD-upwind scheme, i.e., computed after 20 periods on a grid with 160 cells using a CFL number 0.2. As for the central scheme, we can observe the effects of dissipation (for $\tau = 1.0$ and $\tau = 0.5$), compression ($\tau = 0.0$), and overcompression ($\tau = -0.25$). We obtained similar results with a CFL number of 0.4 (note that the non-staggered upwind scheme (28) allows a timestep roughly twice as large as the staggered scheme (2), (7)).

5. APPLICATION TO COMPRESSIBLE GAS DYNAMICS

To demonstrate the potential of compressive limiters for more general systems of conservation laws, we study an example from one-dimensional gas dynamics proposed by Shu and Osher [20]. The example describes a moving Mach 3 shock that interacts with a turbulent
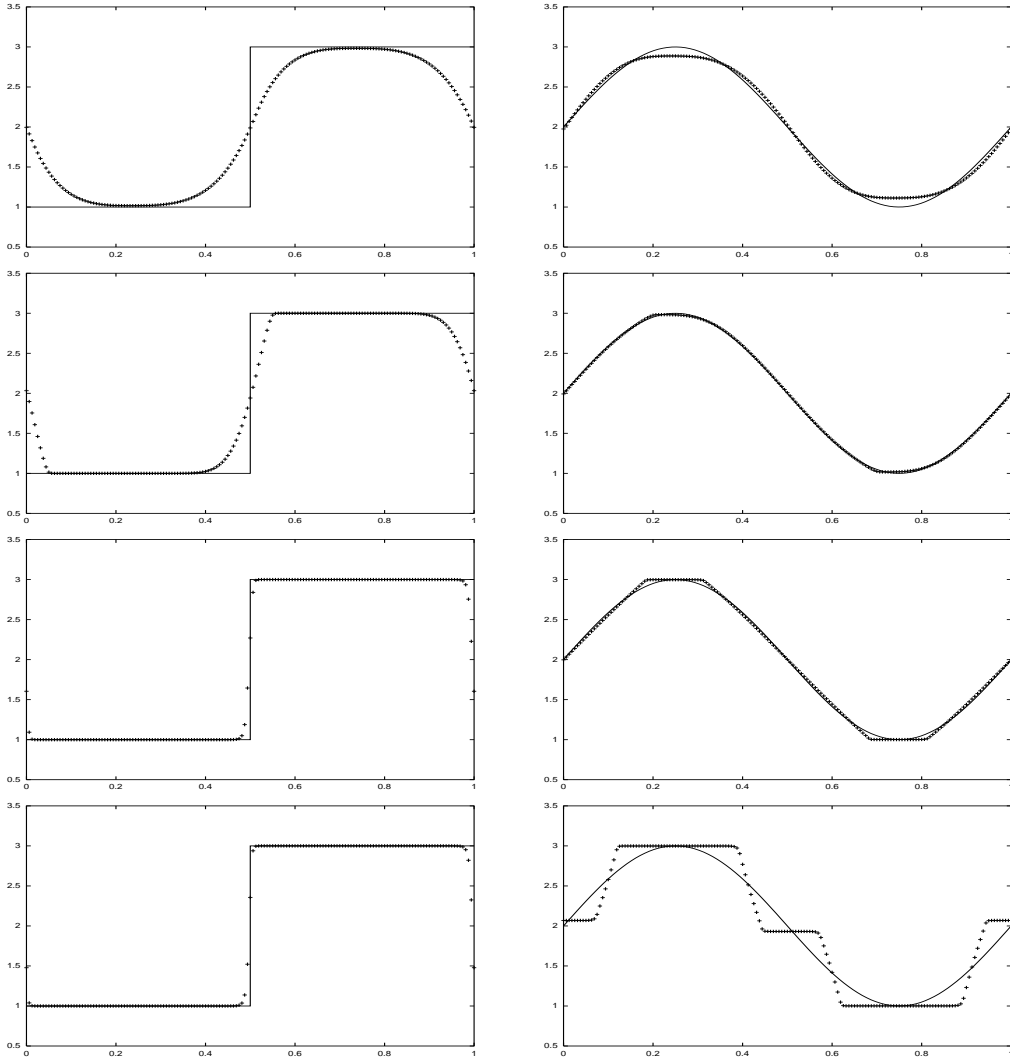
FIGURE 8. Same computation as in Figure 7, but using the TVD-upwind scheme (28).

flow represented by a sine wave in the density. The initial configuration is as follows

$$(29) \qquad (\rho, u, p)(x, 0) = \begin{cases} (3.857143, 2.629369, 10.33333), & x < -4 \\ (1 + 0.2 \sin 5x, 0, 1.0), & x \geq -4. \end{cases}$$

Figure 9 shows the solution at $t = 1.8$ computed on a fine grid over the domain $x \in [-5, 5]$.

In Figures 10 and 11 we show enlarged plots of the density in the preshock and the post-shock region for three approximations computed on a grid with 400 cells using different limiting strategies: (i) the well-balanced van Leer limiter for all waves; (ii) the van Leer limiter for nonlinear waves and the compressive ACM limiter ϕ_2^{ACM} for linear waves using a partial characteristic decomposition (PCD) to separate the linear waves; and (iii) the compressive limiter ϕ_2^{ACM} for all waves. The second strategy exhibits the stability observed for the van Leer scheme for the nonlinear waves (the three leftmost saw-tooth patterns) and at the same time captures the extremities of the complex linear-nonlinear wave pattern in the rightmost
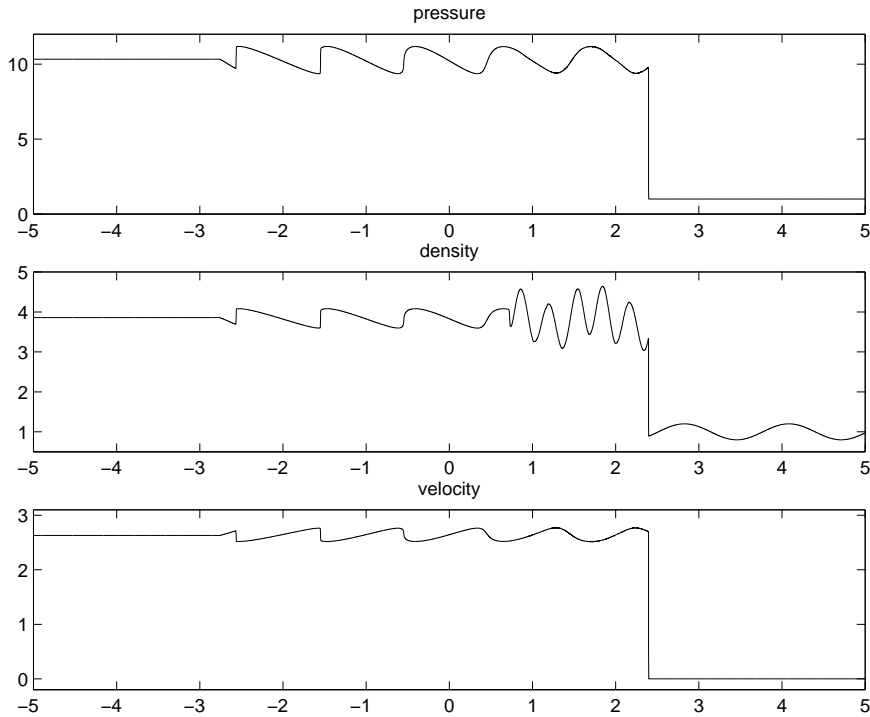
FIGURE 9. Reference solution of the vortex test case computed on a fine grid.

postshock region, which the van Leer computation was not able to resolve. In the preshock region, the PCD based scheme shows a slight tendency of sharpening the smooth sine waves but does not decrease the extreme values as the van Leer limiter does. Note also that using a compressive limiter on all waves slightly disturbs the smoothness of the nonlinear wave for $x \in [0, 0.5]$. This does not occur when using the PCD and applying compression only to the linear wave.

Judging from Figures 10 and 11, ACM on all waves seems to give better resolution than using van Leer on this particular grid. However, a grid refinement study reveals that on finer grids, the ACM limiter overcompresses the smooth, nonlinear waves in the postshock zone into staircase waves (see Figure 12). This shows that rarefaction waves cannot spread at the physically correct rate. Ultimately, such overcompression may lead to entropy violating shocks. This is clear evidence that compressive limiters should not be applied to the nonlinear fields. The PCD strategy, on the other hand, does not overcompress the nonlinear waves, and gives improved resolution compared with van Leer's limiter: using 400 points, the PCD strategy resolves the peaks behind the leading shock as well as using 800 points and applying van Leer's limiter to all waves. With PCD and 800 points, the peaks are fully resolved, and there is only marginal overcompression of the sine-waves ahead of the shock. In Table 1 we give the relative errors in primitive variables for the grid refinement study.

In [14] we have applied the artificial compression techniques to the two-dimensional system of compressible gas dynamics. ACM enabled us to improve the resolution of contact waves and small vortices dramatically, but it did also create spurious oscillations when too much compression was added.
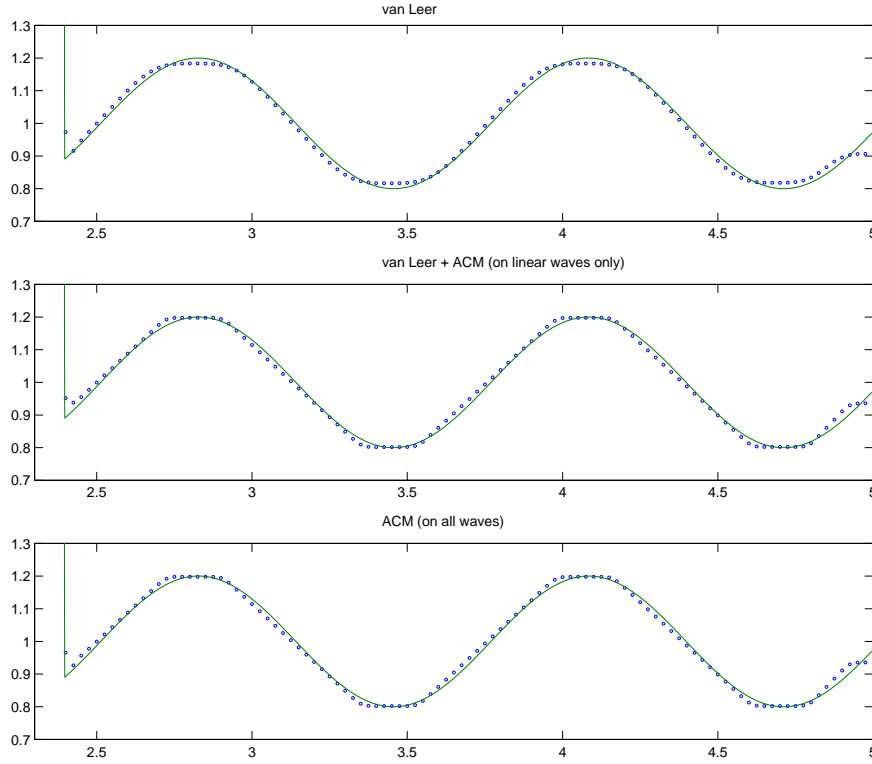
FIGURE 10. Comparison of density approximations computed on a 400 cell grid by the three different limiting strategies, zoom on the preshock zone.

TABLE 1. Grid refinement study for the vortex test case for limiting strategies (i)–(iii); n_x denotes the number of grid cells, and E_q the relative L^1 error of primitive variable q.

|	n_x	E_ρ	E_u	E_p	CPU
(i)	200	2.97e-02	9.54e-03	1.41e-02	0.22
	400	1.86e-02	4.03e-03	5.99e-03	0.89
	800	6.83e-03	2.05e-03	2.85e-03	3.49
	1600	3.04e-03	1.15e-03	1.57e-03	13.90
	3200	1.62e-03	6.14e-04	9.50e-04	67.30
(ii)	200	2.68e-02	7.83e-03	1.27e-02	0.42
	400	1.07e-02	3.69e-03	5.74e-03	1.65
	800	4.28e-03	1.91e-03	2.74e-03	6.18
	1600	2.32e-03	9.65e-04	1.32e-03	25.00
	3200	1.26e-03	4.41e-04	6.47e-04	111.00
(iii)	200	2.55e-02	6.05e-03	9.46e-03	0.23
	400	1.16e-02	4.86e-03	7.74e-03	0.98
	800	7.74e-03	2.96e-03	4.56e-03	3.81
	1600	4.72e-03	1.53e-03	2.34e-03	15.60
	3200	3.01e-03	1.04e-03	1.74e-03	70.10
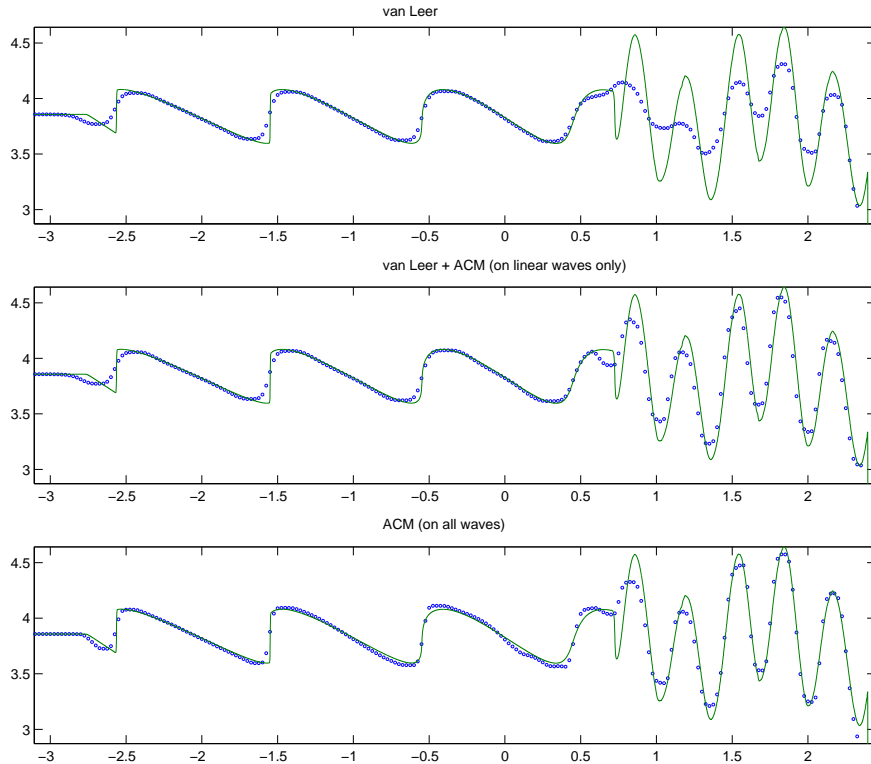
FIGURE 11. Comparison of density approximations computed on a 400 cell grid by the three different limiting strategies, zoom on the postshock zone.

6. CONCLUSION

In this paper, we have investigated Harten's ACM as a technique to sharpen linear discontinuities computed by the staggered central scheme of Nessyahu and Tadmor. For the prototype linear advection equation, Harten's ACM reduces to a limiter of the family analyzed by Sweby [21]. A rigorous TVD analysis allows us to derive reconstructions which are much more compressive than Harten's ACM. Similarly as for the upwind schemes considered by Sweby, we show that central schemes using compressive limiters may overcompress smooth linear waves into piecewise linear ones or even into step functions. They may also prevent the correct spreading of rarefaction waves for nonlinear fields. We conjecture that a single parameter may be used to classify Sweby-type limiters as dissipative, well-balanced, compressive and over-compressive. Numerical experiments with a new family of limiters back up the suggested classification both for central and for upwind schemes.

Here are some guidelines derived from the analysis and experiments of this paper: usually, one should rely on a well-balanced limiter (in the sense of Classification 6 above) like MinMod2 (17) or van Leer (18). Computations with compressive limiters like Superbee (19), our new ACM limiter (26) or our modified Superbee limiter (27) may improve the resolution of linear discontinuities dramatically, but should be checked carefully to exclude overcompression. As a general rule, one should not apply compressive limiters to evolving rarefaction waves.

Let us briefly discuss piecewise linear reconstructions beyond those considered by Sweby. Sweby-type limiters are based on the ratio of consecutive differences of the cell-averages
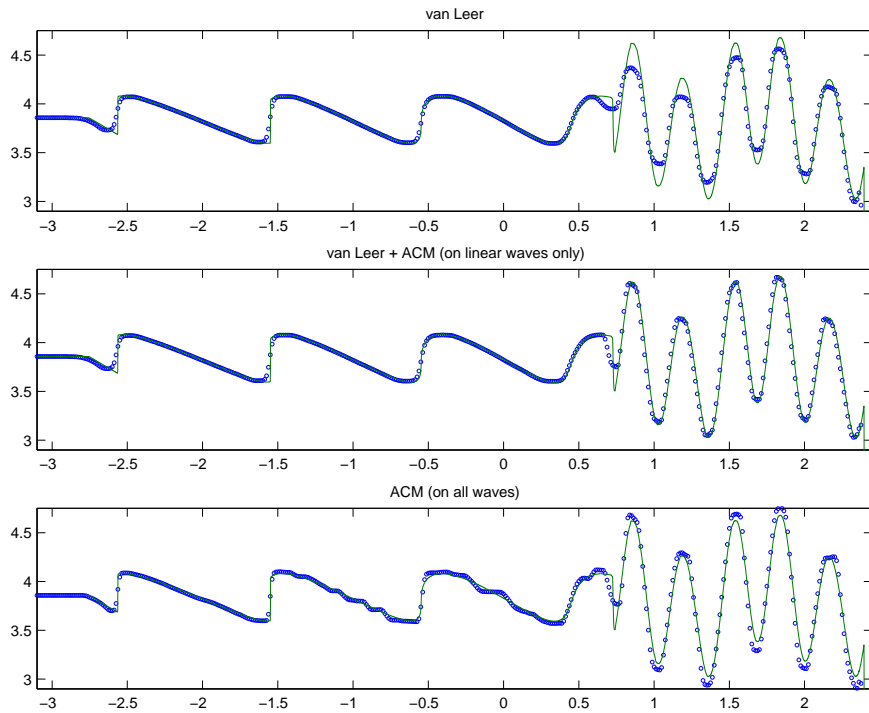
FIGURE 12. Comparison of density approximations computed on a 800 cell grid by the three different limiting strategies, zoom on the postshock zone.

of the numerical solution, $r_i = (u_{i+1} - u_i)/(u_i - u_{i-1})$. This ratio does not distinguish between corners of a step function, where compression is desirable, and smooth extrema, which should not be compressed. A more sophisticated class of reconstructions should use additional information like a local smoothness indicator or error estimator. This information might then be used to select the appropriate Sweby-type limiter. First experiments in this direction are promising, and we hope to report on them in due time.

REFERENCES

[1] P. Arminjon, D. Stanescu and M.-C. Viallon. A two-dimensional finite volume extension of the Lax–Friedrichs and Nessyahu–Tadmor schemes for compressible flows. *Proc. 6th. Int. Symp. on CFD, Lake Tahoe* M. Hafez and K. Oshima (eds.), Vol. IV, pp. 7–14, 1995.

[2] P. Arminjon and M.-C. Viallon. Convergence of a finite volume extension of the Nessyahu–Tadmor scheme on unstructured grids for a two-dimensional linear hyperbolic equation. *SIAM J. Numer. Anal.* 36(3):738–771, 1999.

[3] P. Arminjon, M.-C. Viallon and A. Madrane. A finite volume extension of the Lax–Friedrichs and Nessyahu–Tadmor schemes for conservation laws on unstructured grids. *Int. J. Comput. Fluid Dyn.* 9(1):1–22, 1997.

[4] S. K. Godunov. A finite difference method for the computation of discontinuous solutions of the equations of fluid dynamics. *Mat. Sb.*, 47:357–393, 1959.

[5] A. Harten. The artificial compression method for computation of shocks and contact discontinuities. III. Self-adjusting hybrid schemes. *Math. Comp.*, 32(142):363–389, 1978.

[6] A. Harten. High resolution schemes for hyperbolic conservation laws. *J. Comput. Phys.*, 49:357–393, 1983.

[7] G.-S. Jiang and E. Tadmor. Nonoscillatory central schemes for multidimensional hyperbolic conservation laws. *SIAM J. Sci. Comput.*, 19(6):1892–1917 (electronic), 1998.

[8] A. Kurganov, S. Noelle and G. Petrova. Semi-discrete central-upwind schemes for hyperbolic conservation laws and Hamilton-Jacobi equations. *SIAM J. Sci. Comp.* 23(3):707–740, 2001.

[9] A. Kurganov and G. Petrova. Central schemes and contact discontinuities. *Math. Model. Numer. Anal. (M2AN)*, 34:1259–1275, 2000.

[10] A. Kurganov and E. Tadmor. New high-resolution central schemes for nonlinear conservation laws and convection–diffusion equations. *J. Comp. Phys.*, 160:214–282, 2000.

[11] P. Lax. Weak solutions of nonlinear hyperbolic equations and their numerical computation. *Comm. Pure Appl. Math.*, 7:159–193, 1954.

[12] R. LeVeque. Numerical Methods for conservation laws. 2nd edition, *Birkhäuser* (1992).

[13] D. Levy, G. Puppo, G. Russo. Compact central WENO schemes for multidimensional conservation laws. *SIAM J. Sci. Comp.*, 22:656–672, 2000.

[14] K.-A. Lie and S. Noelle. High resolution nonoscillatory central difference schemes for the 2D Euler equations via artificial compression. In "Progress in Industrial Mathematics at ECMI 2000", M. Anile, V. Capasso, and A. Greco (eds.), *Mathematics in Industry*, Vol. 1, Springer Verlag, 2002.

[15] S. F. Liotta, V. Romano and G. Russo. Central schemes for balance laws of relaxation type. *SIAM J. Numer. Anal.* 38:1337–1356, 2000.

[16] X.-D. Liu and E. Tadmor. Third order nonoscillatory central scheme for hyperbolic conservation laws. *Numer. Math.* 79:397–425, 1999.

[17] H. Nessyahu and E. Tadmor. Non-oscillatory central differencing for hyperbolic conservation laws. *J. Comput. Phys.* 87:408–463, 1990.

[18] P. Roe. Approximate Riemann solvers, parameter vectors, and difference schemes. *J. Comput. Phys.*, 43:357–372, 1981.

[19] V. Romano and G. Russo. Numerical solution for hydrodynamic models of semiconductors. *Math. Models Meth. Appl. Sc.* 10:1099–1120, 2000.

[20] C.-W. Shu and S. Osher. Efficient implementation of essentially non-oscillatory shock-capturing schemes, II. *J. Comput. Phys*, 83:32–78, 1989.

[21] P. K. Sweby. High resolution schemes using flux limiters for hyperbolic conservation laws. *SIAM J. Numer. Anal.*, 21:995–1011, 1984.

[22] Y. C. Tai, S. Noelle, N. Gray and K. Hutter. Shock capturing and front tracking methods for granular avalanches. *J. Comput. Phys* 175:269-301, 2002.

[23] B. van Leer. Towards the ultimate conservative difference scheme V. A second order sequel to Godunov's method. *J. Comput. Phys.*, 32:101–136, 1979.

(Knut–Andreas Lie)
SINTEF APPLIED MATHEMATICS,
P.0. BOX 124 BLINDERN, N–0314 OSLO, NORWAY
ALSO: DEPARTMENT OF INFORMATICS, UNIVERSITY OF OSLO
   E-mail address: Knut-Andreas.Lie@math.sintef.no
   URL: http://www.ifi.uio.no/~kalie/

(Sebastian Noelle)
INSTITUT FÜR GEOMETRIE UND PRAKTISCHE MATHEMATIK,
RWTH AACHEN, 52056 AACHEN, GERMANY
   E-mail address: noelle@igpm.rwth-aachen.de
   URL: http://www.igpm.rwth-aachen.de/~noelle/